The challenges of using satellite data sets to assess historical land use change and associated greenhouse gas emissions: a case study of three Indonesian provinces

Article

Accepted Version

The challenges of using satellite datasets to assess historical land use change and associated greenhouse gas emissions - a case study of three Indonesian provinces

Advances in satellite remote sensing and the wealth of earth observation (EO) data now available have improved efforts towards determining and quantifying historical land use and land cover (LULC) change. Satellite imagery can overcome the absence of accurate records of historical land use, however the variability observed in the case study regions demonstrates a number of current challenges.

Differences in spatial coverage, resolution and land cover classification can lead to challenges in analysing historical LULC datasets to estimate LULC change and associated greenhouse gas (GHG) emissions. This paper demonstrates the calculation of LULC change from three existing, open source LULC datasets to show how this can lead to significant variation in estimates of GHG emissions related to differences in land classification methodologies, Earth Observation (EO) input data and period of investigation. We focus on selected regions of Indonesia, where quantifying land use change is important for GHG assessments of agricultural commodities and for evidencing progress against corporate and government deforestation commitments.

Given the significance of GHG emissions arising from LULC change and the increasing need for emissions monitoring, this research highlights a need for consensus building to develop consistency in historic and future LULC change estimates. This paper concludes with a set of recommendations for improvements to ensure consistent LULC mapping.

Keywords: land use/ land cover change, GHG emissions, remote sensing, palm oil, sustainability,

Introduction

Advances in satellite remote sensing (RS) and the wealth of earth observation (EO) data now available have improved efforts towards accurately mapping Land Use and Land Cover (LULC) and quantifying change [1]. This reduces reliance on e.g. ground-level monitoring and improves the resolution of assessments that are currently based on country-level statistics. However, challenges remain, and factors such as the type of data (e.g. optical or radar) and spatial and temporal resolution of satellite data may significantly influence the classification of land use and land cover [1,2]. Several organisations have produced and made openly available LULC datasets based upon the interpretation of optical EO satellite data. These are derived from different satellites, based on different sensors, with variations in return time and LULC classification methodology. In this paper, we analyse uncertainty in greenhouse gas (GHG) emission estimates by calculating LULC change with three historic LULC datasets, with a focus on selected regions of Indonesia where the development of the Palm Oil (PO) industry has been a significant driver of LULC change in recent decades [2].

LULC mapping

Mapping of LULC is one of the key applications of RS technologies and has been carried out for at least 40 years [3]. However, there is little agreement on best practice for LULC mapping. A recent overview of different LULC mapping methodologies is provided by Joshi et al., (2016) [1]. The process of remote sensing image classification is complex and involves many steps, including the determination of a land cover classification system, collection of data sources and selection of a classification algorithm [4]. One of the most important considerations in LULC mapping is the *definition of LULC classes*. This can be done with a focus on Land Use (purpose for which humans use land) or Land Cover (physical properties of a land surface) [1]. LULC class definitions can be either broad (e.g. Forest, Agriculture, Grassland etc.) or specific (e.g. subdividing agricultural land into Oil Palm, Corn, Banana, etc.). Optimal class definition depends on the specific needs of the user, but, in general, broad classes are better suited for large-scale (continental) LULC mapping. Whilst higher specificity in land classes is preferable for regional or national-scale land mapping studies [1], it has been shown that using a large number of highly specific classes can lead to misclassification, as differences between classes become small [5,6].

Another major consideration when developing a LULC classification scheme is the selection of optimal RS input data. Low resolution (LR) optical sensors (e.g. MODIS, MERIS) have been useful for vegetation mapping at global or continental scale, while medium resolution (MR) satellites (e.g. Landsat TM) are most frequently used for regional LULC mapping [4]. High resolution (HR) satellite data (e.g. DigitalGlobe, SPOT) require greater resource in terms of processing capacity and can be costly when large area coverage needs to be acquired. Therefore, HR data is more likely to be used for validation of smaller areas [4]. Quality of RS imagery can be hampered by persistent cloud cover in tropical regions [2]. Integrated use of Synthetic Aperture Radar (SAR) satellite data, which has high resolution capability and is unaffected by cloud cover, has shown to be improving LULC mapping significantly [1] and is becoming more commonly used in tropical LULC mapping [7].

The *classification methodology used for LULC mapping* is a third major consideration. There is a plethora of image classification algorithms and methodologies available [1]. Common methodologies or algorithms range from statistical methods (e.g. Maximum Likelihood Classification (MLC), Principle Component Analysis (PCA)) [8,9], machine learning algorithms (Support Vector Machine (SVM), Random Forest (RF)) [10–12], knowledge-based/decision trees methods [6,13] to visual/manual interpretation of satellite data [12]. Changes in LULC class definitions, RS data input and classification methods over time can lead to issues of consistency and variability in estimates of historical LULC change [2].

GHG emissions attributable to LULC change

Carbon dioxide emissions from fossil fuel use are relatively well quantified, but GHG emissions from LULC change remain highly uncertain and yet are one of the largest anthropogenic sources of GHG emissions [14]. Land-use changes can cause emissions due to carbon losses in both biomass and soils [15]. Rapid expansion of agriculture for large scale commodity crops can lead to large changes in carbon stocks [16].

Understanding emissions from LULC change is key to quantifying life cycle emissions of large scale agricultural commodities, such as PO. Growth in PO production in South-East Asia, led primarily by Indonesia and Malaysia, has been a key component of meeting growing global demand for bio-based oil in recent decades. Indonesia and Malaysia currently meet more than 85% of global PO demand, 51% and 34% respectively [17]. In these countries, plantations cover an estimated area of 140,000 km^2 on both mineral and organic (peat) soils, which has led to large-scale LULC change in the region [2].

A historical record of 20-25 years is necessary for LUC emissions to be included in Life Cycle Assessments (LCA). Openly-available satellite data with global coverage, and of sufficient quality, does not widely exist prior to 2000 and, therefore, this period is rarely covered by LULC datasets.

Significance of peat soils

Soils in wetland ecosystems (e.g. peat swamp forests) contain large amounts of organic material, and therefore have high below-ground carbon stocks with carbon densities that may exceed those of the aboveground vegetation [18]. When organic soils are disturbed, and particularly when drained, removing water from the soil pores; oxygen can enter the soil surface and oxidize the soil organic material through biological and chemical processes. Oxidation of soil organic matter leads to a carbon flux to the atmosphere, mostly as CO_2 [19].

GHG emissions after drainage are not constant; they will vary as water tables and peat characteristics change [20]. In typical PO plantation developments on peat soils in Southeast Asia, the initial peatland drainage usually involves a rapid lowering of the water table to depths of around or below 1 m to over 3 m. In the first few months or years after drainage, the peat surface will change rapidly through a combination of peat oxidation and soil compression. In this transition phase, carbon emissions are higher than during the subsequent, more stable phase i.e. following palm planting, when water levels will generally be maintained at depths of around 0.80 m. From that point onwards, oxidation will proceed at a more or less stable rate until the peat surface is at or close to the local drainage level; dependent upon the peat depth, this may take several decades [20].

Any holistic assessment of the carbon emissions arising from LULC change must include both changes in above- and below-ground carbon stocks. The relative proportion of PO plantations on organic soils in Southeast Asia has increased over the last 20 years; these now occupy some 31,000 km^2, or approximately 23% of the total area under PO plantations [21]. It has been shown that this process has been responsible for generating substantial carbon losses and associated GHG emissions from peat decomposition [19].

Aim of this paper

The aim of this paper is to evaluate and compare existing LULC datasets, derived from EO data, to assess historical LULC change and associated GHG emissions. To achieve this, we focus on three Indonesian provinces where large-scale LULC change has been observed in recent decades, much of which is attributable to the development of plantations.

Materials and methods

Study area

We focus on three areas of interest (AOIs), namely the Indonesian provinces of Northern Sumatra, Riau on the island of Sumatra, and Central Kalimantan on the island of Borneo, Figure 1. These three AOIs, covering approximately one sixth of the total area of Indonesia, lie within an area that is the focus of much attention surrounding land use change emissions [22–24]. All AOIs include areas with peat soils, according to the peat soil map distributed by the Centre for Remote Imaging, Sensing and Processing (CRISP) in Singapore [19]. Additionally, in all three AOIs PO production occurs on both mineral and peat soils, according to PO concession data obtained from Global Forest Watch [25], (Table 1).

LULC data sources

Three open-source, satellite-derived LULC datasets were identified as thematically and spatially relevant for the AOIs, as detailed in Table 2.

The Climate Change Initiative (CCI) LULC dataset was developed by the European Space Agency (ESA) CCI Land Cover Initiative, currently available with updates for the period 1992-2015. CCI is a global LULC dataset, with a class definition based on the Land Cover Classification System (LCCS) developed by the United Nations (UN) Food and Agriculture Organization (FAO) [26]. Class definitions are broad, with no specific LULC classes for tree plantations. Quality assessment of the CCI dataset (included in [26]) was based on referencing using higher resolution satellite data or derived products (Landsat, Google Earth, SPOT-Vegetation (SPOT-VGT)) for specific reference areas, which were chosen to cover all global climatic zones, with subsamples chosen randomly from these areas. The overall accuracy between the CCI 2010 dataset and a reference dataset for 2009 was 74.4%.

The CRISP LULC dataset was developed by the Centre for Remote Imaging, Sensing and Processing in Singapore and covers Southeast Asia, with updates for 2000, 2010 and 2015. The mapping methodology is well documented [21,27]. The 2015 LULC data update has been developed using a methodology which differs significantly from that used for the 2000 and 2010 updates; CRISP have therefore advised users to avoid comparisons of the 2015 data with older updates for LULC change analysis [21]. The class definition is specific, with two classes for plantations ("Large scale palm plantations" and "Plantation/regrowth"). Quality assessment of the CRISP dataset was carried out by comparing the LULC maps with a total of 1000 random sample plots from very-high resolution satellite data [21]. The total accuracy for the 2015 CRISP dataset was 81.6%.

The MoF LULC dataset was developed at the Indonesian Ministry of Forestry, and currently provides irregular updates between 1990 and 2015. In total ten updates are available, of which eight are between 2000 and 2015. There is no accompanying documentation detailing the image classification methodology used for the LULC mapping. However, according to [23], it is primarily based on visual interpretation of Landsat 30x30 m satellite data. There is no indication of whether any quality assurance checks have been carried out. When considering forest cover in Indonesia, comparison between MoF and Global Forest Watch forest cover data [28] indicated agreement in 90.2% of the area considered [29]. The MoF LULC classes are specific, identifying two plantation types (general plantation and timber plantation), as well as undisturbed and disturbed forests.

Data pre-processing

Figure 2 presents an overview of the processing and analysis workflow. After collection of the LULC, AOI boundary and peat soil extent data, the data is pre-processed using the following steps:

- Conversion of LULC data to raster. The MoF data is delivered in vector format, in order to make the dataset comparable in terms of resolution, it was converted to raster with a 100 x 100 m spatial resolution.
- Subsetting of LULC and peat soil data per AOI.
- Split of LULC data between peat soil and non-peat soil areas.
- Reprojection of data to the same Universal Transvers Mercator (UTM) zone projection, UTM 47N for North Sumatra and Riau AOI data, UTM 49N for Central Kalimantan.
- Class aggregation of specific LULC classes into broad classes for the cross-comparison of LULC data, detailed below.

Cross-comparison LULC data

Pairwise comparison of the three LULC datasets was carried out using the Mapcurves analysis [30]. Mapcurves analysis provides a method to compare two categorised maps by cross-referencing, to quantify the similarity between the classifications. This analysis provides insight by calculating the proportion of overlap between each LULC class from one dataset (Map A) and the best overlapping LULC class from another dataset (Map B). The best overlaps for all classes from Map A with classes from Map B are calculated, and the overlap fractions are summed to derive the total agreement between Map A and Map B. This total is named the Goodness of Fit (GoF); a GoF of 1.0 means a perfect fit, a GoF of 0.0 no fit at all. This analysis can be run both ways, i.e. using map

A as the original and using Map B as the reference, or vice versa. The GoF is expressed as a percentage and can therefore be compared across categories and maps.

It should be noted that the GoF does not give information about the total area of agreement, as each LULC class has equal influence on the GoF, regardless of its area of presence in the original map. Nor does this analysis provide insight into relative quality of datasets, but gives an indication of the proportion of overlap.

To make the three LULC datasets as comparable as possible, LULC classes were aggregated into nine broad classes, based on a general class aggregation utilised for the CCI data [26]: Agriculture, Forest, Grassland, Shrubland, Sparse Vegetation, Wetland, Settlement, Bare and Water.

The cross-comparison analysis was run for dates pertaining to two specific years in which all three LULC datasets have an update, 2000 and 2015 (Figure 3a-f).

LULC change analysis

To calculate LULC change for each LULC dataset, changes between each initial update (t0) to the next update (t1) were calculated from the pre-processed data. This was done by comparing each pixel location from the t0 raster data with each corresponding pixel from the t1 data. If a change in LULC class was observed, the pixel was reclassed as a pixel with a unique value combining the t0 and t1 class code. If no change was observed, the pixel was reclassed as no value, see Figure SM1. From this analysis, LULC change maps and tables were produced. Table SM1 provides the time periods used to assess LULC change. For CCI and MoF, these time periods coincide with the updates of the MoF dataset, for CRISP only one period has been used, 2000 to 2010, as the update of CRISP for 2015 cannot be compared for LULC change analysis [21]. The

LULC change is expressed in hectares per year, to correct for varying time intervals between updates.

Carbon emission modelling

To convert LULC change into carbon emission estimates, values for Aboveground Biomass (AGB) and Organic Soil Degradation (OSD) emissions factors were obtained for all the LULC classes of the three datasets. This was done by conducting a review of published literature related to LULC change in Southeast Asia (primarily based on [15,20,31–33]). From this review, average values for AGB and OSD for each LULC class were calculated (Table SM2 and Table SM3). AGB emission factors are expressed in Mg C ha^{-1}, the OSD emissions are given in Mg C ha^{-1} yr^{-1}, as these continue for an indefinite period after a LULC change from natural to man-made state [19]. The LULC change data from the selected areas and the AGB and OSD emission values were combined to estimate GHG emissions. The model, Equation 1, is a simplified version of the model in [34], not taking into account the GHG emissions related to peat fire due to additional uncertainty.

$$E = E_a - S_a + E_{bo} \tag{1}$$

where E is the emission estimate, E_a is emission from AGB due to LUC, S_a sequestration of CO_2 from the atmosphere into crop biomass between succeeding land uses and E_{bo} is emission from OSD. A graphical example of the model is provided in Figure SM2. For example, if 1 ha changes from Primary Forest (average AGB 233 Mg C ha^{-1}) to Shrubland (average AGB 31 Mg C ha^{-1}) then, for AGB, a total of 233-31 = 202 Mg C will be emitted. If subsequently this 1 ha of Shrubland becomes Plantation (average AGB 37 Mg C ha^{-1}) then the net carbon emissions will be 31-37 = -6 Mg C, which indicates carbon sequestration.

The latest insights with respect to emissions from drained peatlands are reported by IPCC [20,35]. The OSD emission factor values used in this paper relate to ongoing oxidation of peat. We exclude additional emissions occurring during the first 5 years after drainage for plantation establishment [20,36], relating to fires [37], and the potential emissions from organic carbon flushed into aquatic ecosystems (e.g. as dissolved organic carbon (DOC), and associated emissions of CO_2 and CH_4 [38]). These emissions are highly uncertain and would, therefore, obscure the uncertainty in GHG estimates from different LULC datasets. Thus, in our calculations, if Peatswamp Forest on organic soil changes to PO Plantation, the OSD emission related to land conversion is 11 Mg C ha^{-1} yr^{-1}.

On the basis of [31], who reported that, for mineral soils, the net temporal trend in the soil carbon stock (in the top 30 cm of soil) was not significantly different from zero in both forest- and non-forest-derived plantations, we assume soil carbon stock neutrality on mineral soils used for oil palm cultivation.

Results and discussion

Cross-comparison LULC data (Mapcurves)

The Mapcurve plots with the highest consistencies for each area and date are visualised in Figure 3. The highest GoF values are observed for either a combination of CCI as Original and CRISP as Reference map or the combination of MoF as Original and CRISP as Reference map. The highest GoF observed is 0.575 for North Sumatra in 2015, by combining MoF and CRISP, which means there is 57.5% class agreement between these maps. All other combinations lead to lower GoF values (see Tables SM4 and Table SM5). The two data types most dissimilar are the MoF and CCI datasets (generally less than 40% class agreement).

The Mapcurve analysis shows large inconsistencies between LULC datasets, even after aggregation of specific LULC classes, to make the datasets more comparable. Other comparative studies of LULC datasets have also observed this [39–41], either by means of the Mapcurves analysis, or by analysing spatial overlap of similar classes on a pixel-by-pixel basis. Of these studies, the maximum observed Mapcurve value was 0.53 [41], while in a pixel-by-pixel based analysis the highest agreement was found to be 62% [40]. This shows that, even after aggregation of specific LULC classes into broader classes, high levels of agreement between LULC maps of similar age cannot be assumed.

Differences between LULC maps can be caused by a number of factors [42], including data quality, spatial and temporal resolution, LULC classification approaches, algorithms and aggregation. Data quality can be limited in tropical regions, due to persistent cloud cover and therefore a limited number of useful satellite acquisitions. If sufficient temporal resolution is available, there is better chance that high quality imagery can be obtained in a certain period.

Spatial resolution dictates the smallest mapping unit. In general, if a pixel is sufficiently small, more specific LULC can be distinguished. Lower spatial resolution pixels often cover more than one specific LULC class, and therefore the LULC class definition must be more generic, as for CCI. Spectral resolution influences how well LULC classes can be technically distinguished. MODIS data, which underlies the CRISP dataset, operates in 34 spectral bands [43], whereas Landsat-8 operates in 11 bands [44]. This means that even though MODIS has a spatially lower resolution than Landsat, through its superior spectral resolution, MODIS might be able to detect more subtle variations in LULC than Landsat.

As noted above, a several classification algorithms were used to develop the LULC datasets, which have an effect on differences in mapping results. In general, pixel-based classifiers tend to lead to high heterogeneity in the resulting LULC map, as each pixel is individually classified. Therefore, it is currently more common to include a clustering step in the classification process, as this has been found to positively influence the map accuracy [45,46]. The MoF dataset is based on visual interpretation of satellite data, which depends on the interpretation skills of each person working on the LULC maps, which can be subjective [47]. LULC class definition can impact how readily LULC datasets can be compared. Aggregation of specific LULC classes into broad classes can overcome this problem to a large extent, although it is not always clear to which broad class a specific class might belong.

LULC change

For each LULC dataset, LULC change has been calculated for each period between updates (shown in Table SM3). The LULC change observed in each area is presented for North Sumatra (Figure 4), Riau (Figure 5) and Central Kalimantan (Figure 6), The LULC change is averaged to give LULC change in hectares per year, to make the differing periods between updates directly comparable.

According to the MoF dataset, for each AOI, one ‘peak change period’ with an extreme LULC change is recorded. In North Sumatra this is 2006-2009, 2012-2013 in Riau, and 2013-2015 in Central Kalimantan. From the data (Table SM6), the North Sumatra peak change period is 4.7 times larger than the average for 2000-2015, 2.5 times larger than average for the Riau peak change period and 3.8 times larger than the average in Central

Kalimantan. It is questionable whether these changes, visible in the RS data, are related to ‘actual observed’ LULC change in the AOI, which we define as change that can be seen at ground level (corroborated by field observations), or have other causes. Table 3 shows the largest contributors to these peak change periods, according to the MoF datasets. Analysis shows that for each occurrence the MoF class ‘Dry Rice Land Mixed with Scrub’ was involved, either by transition from this class to ‘Dry Rice Land’ (in North Sumatra) or transition into it from ‘Scrubland’ (both Riau and Central Kalimantan). The class ‘Dry Rice Land Mixed with Scrub’ can be interpreted as a transition class between Rice Land and Scrubland, or an ecotone. Defining class boundaries for ecotones is often difficult when making observations in the field; it is even more challenging when interpreting RS data [48]. Due to the magnitude of these peak change periods, it is unlikely that they are related to actual changes in LULC, but more likely related to different interpretation of RS data or methodological shift between MoF updates. However, the influence of this mapping effect on the LULC change observed in Central Kalimantan in 2013-2015 is relatively small, and the majority of LULC change estimated for this period can be attributed to ‘actual observed’ LULC change at ground level.

The CRISP maps consistently give higher estimates for land use change than either the CCI or MoF maps. The annual LULC change estimated by CRISP is between 6.1 and 12.8 times larger than the LULC change from CCI for the AOIs. For CRISP to MoF, the difference ratios for LULC change lie between 2.2 and 3.8.

Temporal correlations between MoF and CCI data are plotted in Figure 7. As CRISP only provides one update (between 2000 and 2010) this dataset has not been included. The MoF LULC change values have been corrected for the peak change periods described above, to get a better comparison of actual observed LULC change between

CCI and MoF datasets. The strongest temporal correlation is shown in North Sumatra, with an R^2-value of 0.7978, while those for Riau and Central Kalimantan are much lower.

The LULC change analysis shows little agreement between LULC datasets in the AOIs. Whilst some inconsistency can be attributed to methodological factors, not all can be explained directly.

GHG Emissions

Large variability in GHG emissions can be observed for estimates made using the different LULC datasets, Table 4 and Table 5 (see also Figure SM3, Figure SM4 and Figure SM5). GHG emissions estimates from CRISP data (2000-2010 only) are considerably higher than those from both CCI and MoF data, while those from MoF for the period 2011-2015 are generally much higher than the estimates from CCI (Table 5). For Riau and Central Kalimantan, this is partly due to the MoF data inconsistency related to the classification of ‘Scrubland’ and ‘Dry Rice Land Mixed with Scrub’. The peak change periods are also visible, with a peak in emissions in Riau in 2012-2013 (Figure SM4) and in Central Kalimantan in 2013-2015 (Figure SM5).

These results, which illustrate considerable variability in GHG emission estimates from the different LULC datasets, are supported by other studies, e.g. Agus et al. (2010) [34], estimated that carbon emissions from LULC change studies related to the PO industry in Kalimantan differed by a factor of 4.7.

GHG emission maps

The GHG emission estimates per dataset, area and time period can also be displayed geographically in maps of GHG emissions (Figure 8). The highest modelled GHG emissions occur in areas with peat soils, primarily in Riau and Central Kalimantan. However, there are also regions where net carbon sequestration occurs, likely related to conversion of low biomass LULC (bare areas, shrub), to higher biomass LULC (plantations). Bare and shrubland areas may be the result of previous deforestation, which highlights the need for sufficient historic data to understand and account for emissions from LULC change over a longer period, especially in peat soil areas. Several methods exist to attribute these emissions to a product, depending on the data available [49]. For LCA, the impact of land use change should include all direct land use change occurring 20 years (or one full harvest, whichever is longer) prior to the assessment. The total GHG emissions (or removals) arising from LULC change over this period would be allocated equally to each year of the period [50].

Carbon emission factors

The values for emissions from AGB and OSD, derived from literature, are key to the GHG emissions calculations in this study. For plantations, the AGB value used in this study is 37 Mg C/ha, based on a time-averaged value for AGB [15]. However, AGB values of 57.5 Mg C/ha have been reported for plantations at full maturity [51]. To understand this sensitivity, results were calculated using this value (Table SM7). In all but one instance, annual emissions are reduced by 1%- 33% when using the higher carbon stock value for plantation classes. In one case emissions increase (MoF, 2011-2015 for North Sumatra) because a large area of plantation was converted to a LULC with lower carbon stock.

Temporal interval

The results are also sensitive to the interval period used between LULC map updates. This has an impact on GHG emissions related to OSD. It has been shown that emissions from OSD can continue for an indefinite time period after conversion from a natural to man-made state [20]. This process is sketched in Figure SM2, where emissions related to soil degradation from the first stage of LUC continue into the second stage of LUC. It has been observed that when OSD emissions from a previous period are not included, GHG emissions can vary significantly. This has been analysed with CCI data for Central Kalimantan, where GHG estimates derived for 5-yearly intervals (2000-2005 and 2005-2010) were found to be approximately 1 million Mg C/yr higher than emissions summed at intervals of 1 year, over the same 10-year period. This shows the GHG emission model should incorporate LULC changes on organic soils predating the period of interest wherever possible.

Limitations in estimating GHG emissions

The GHG emission estimates were calculated based on published carbon stock and emission factors for different LULC classes. Variability and uncertainty in carbon stocks can be observed in the range of literature values (Table SM2 and Table SM3) arising from influences including of soil type and climate, or where different studies include different elements of carbon pools [15]. Furthermore, peat soils may vary in depth and volume and therefore influence carbon stocks [52]. Since the purpose of this study was to establish uncertainty in GHG estimates resulting from the use of different LULC products, variability and uncertainty in carbon stock values for different LULC classes were not considered further.

Further work could be done to integrate variabilities in carbon stock accounting with the variabilities in estimated LULC changes estimated in this study. Key considerations would include spatial heterogeneity (edge effects) in above and belowground carbon stocks within land cover classes [50, 51]; variability in water table depth and carbon loss rates for OSD [20] and; uncertainties in emissions from land clearance fires on peat soils

[19]. Emissions from degraded peat soils are known to continue a long period, often longer than a typical LCA analysis period of 20-25 years [52]. Therefore, wherever possible, it is advised to incorporate any known historic LULC changes on peat soils for a period as long as possible.

The finding that LULC maps based on RS data interpretation differ is not new [40,41], and some attempts have been made to improve comparability between LULC maps [39]. A LULC dataset is always a trade-off between the input data quality and accessibility, requirements of end-users and the technological and financial means available for development. Each of these datasets represents a valuable source of spatially explicit information for calculating GHG emissions related to LULC change. The current variability between LULC maps suggests that estimates should be used to provide a range rather than a single value for GHG emissions.

Conclusions & recommendations

The need to quantify GHG emissions associated with LULC change is important for life cycle assessments (LCA) of agricultural commodities and for providing evidence of GHG reductions associated with zero net deforestation commitments. Without RS data, such calculations would require detailed historical land records, and therefore these datasets are valuable to estimate regional trends in LULC change and associated GHG emissions. However, this study has shown the potential variability in estimates that can be obtained through use of three open source RS datasets. These variabilities arise from differences in EO input data, land classification methodologies, data resolution and period of investigation. It is therefore advisable to compare different LULC datasets in parallel and use the variability between GHG emission estimates as a confidence interval, rather than a single value. Users should be aware of the potential for variability in LULC estimates.

GHG emission maps, such as Figure 8, are useful visualisation tools that are not commonly available and can provide spatial insight into LULC change and related carbon emissions or sequestration. Current web-based platforms may show forest loss or LULC for a given period, but, to our knowledge, do not yet provide maps showing associated GHG emissions. Given the inconsistencies highlighted in this paper, there is a need for further work to ensure the maps provide robust estimates of LULC change and associated emissions.

The method described in this paper can be used to provide spatially-improved estimates of LULC change and GHG emissions, particularly where the change occurs between LULC types with significantly different carbon stock values, such as between primary forest and plantation. For this to be most effective, there is a need for consensus building and harmonisation on how to develop a consistent and robust approach to assessing historic LULC change, to provide evidence for zero net deforestation commitments, and refine GHG assessments.

We propose the following recommendations to improve LULC mapping for GHG emission estimates for agricultural commodities:

Firstly, the LULC class definition should focus on LULC classes closely associated with the main drivers of LULC change in the AOI. This should include at least the following classes: primary & secondary forest, several types of plantation (where applicable), bare land and cropland. Global LULC datasets often use class definitions that are too broad or lack specific class distinctions important for GHG modelling. Additionally, class definitions of different LULC data sets should be more comparable. The FAO LCCS definitions are developed to be globally relevant and flexible enough to suit most environments [55]. The CCI classes are based on LCCS, it could be useful for other organisations involved in land cover mapping to adopt this system as well.

Secondly and ideally, maps should be updated at least every 2-3 years, and annual updates would be preferable, to capture rapid changes, such as deforestation (fire or logging), bare land, and plantation development.

Thirdly, to enable LULC change analysis over time, mapping methodology should remain unchanged (a period of 20-25 years is required for LCA). If, for example, better mapping algorithms are developed, such that the methodology can be improved significantly, it would be preferable to reprocess the historic data to the new methodology to maintain consistency.

Fourthly, optimal spatial resolution is dependent on the requirements of the user; research on a provincial level can be done at lower spatial resolution than at smaller scale, for example at plantation level. For studies related to a specific agri-food industry it is often sufficient to focus on datasets with a spatial coverage of the main producing areas.

Finally, metadata including quality and methodological information should be published with the datasets.

When the three LULC datasets are compared against these recommendations, it is clear there is currently room for improvement. Signs of improvements are visible, as the recent reprocessing of the European Space Agency's CCI Land Cover initiative has shown. As RS capabilities are advancing quickly and the importance of LULC change analysis is becoming better recognised, this is an excellent time to address these recommendations to make LULC data an even more valuable resource for environmental monitoring.

References

1. Joshi N, Baumann M, Ehammer A, *et al.* A review of the application of optical and radar remote sensing data fusion to land use mapping and monitoring. *Remote Sens.* 8(1), 1–23 (2016).

2. Carlson KM, Curran LM, Ratnasari D, *et al.* Committed carbon emissions, deforestation, and community land conversion from oil palm plantation expansion in West Kalimantan, Indonesia. *Proc. Natl. Acad. Sci.* [Internet]. 109(19), 7559–7564 (2012). Available from: http://www.pnas.org/cgi/doi/10.1073/pnas.1200452109.

3. Anderson JR. A land use and land cover classification system for use with remote sensor data. US Government Printing Office.

4. Kim C. Land use classification and land use change analysis using satellite images in Lombok Island, Indonesia. *Forest Sci. Technol.* [Internet]. 12(4), 183–191 (2016). Available from: http://dx.doi.org/10.1080/21580103.2016.1147498.

5. Srivastava PK, Han D, Rico-Ramirez MA, Bray M, Islam T. Selection of classification techniques for land use/land cover change investigation. *Adv. Sp. Res.* [Internet]. 50(9), 1250–1265 (2012). Available from: http://www.sciencedirect.com/science/article/pii/S0273117712004218.

6. Kuenzer C, van Beijma S, Gessner U, Dech S. Land surface dynamics and environmental challenges of the Niger Delta, Africa: Remote sensing-based analyses spanning three decades (1986-2013). *Appl. Geogr.* (2014).

7. Sameen MI, Nahhas FH, Buraihi FH, Pradhan B, Shariff ARBM. A refined classification approach by integrating Landsat Operational Land Imager (OLI) and RADARSAT-2 imagery for land-use and land-cover mapping in a tropical area. *Int. J. Remote Sens.* [Internet]. 37(10), 2358–2375 (2016). Available from: http://dx.doi.org/10.1080/01431161.2016.1176273.

8. Okamoto K, Kawashima H. Estimation of rice-planted area in the tropical zone using a combination of optical and microwave satellite sensor data. *Int. J. Remote Sens.* (1999).

9. Erasmi S, Twele a. Regional land cover mapping in the humid tropics using combined optical and SAR satellite dataa case study from Central Sulawesi,

Indonesia. *Int. J. Remote Sens.* [Internet]. 30(10), 2465--2478 ST-- Regional land cover mapping in th (2009). Available from: http://www.tandfonline.com/doi/abs/10.1080/01431160802552728.

10. van Beijma S, Comber A, Lamb A. Random forest classification of salt marsh vegetation habitats using quad-polarimetric airborne SAR, elevation and optical RS data. *Remote Sens. Environ.* [Internet]. 149, 118–129 (2014). Available from: http://www.sciencedirect.com/science/article/pii/S0034425714001485.

11. Dong J, Xiao X, Sheldon S, Biradar C, Xie G. Mapping tropical forests and rubber plantations in complex landscapes by integrating PALSAR and MODIS imagery. *ISPRS J. Photogramm. Remote Sens.* (2012).

12. Balzter H, Cole B, Thiel C, Schmullius C. Mapping CORINE land cover from Sentinel-1A SAR and SRTM digital elevation model data using random forests. *Remote Sens.* 7(11), 14876–14898 (2015).

13. Haack BN, Herold ND, Bechdol M a. Radar and Optical Data Integration for Land-Use / Land-Cover Mapping. *Photogramm. Eng. Remote Sensing*. (2000).

14. Maria Roman-Cuesta R, Rufino M, Herold M, *et al.* Hotspots of gross emissions from the land use sector: Patterns, uncertainties, and leading emission sources for the period 2000-2005 in the tropics. *Biogeosciences*. 13(14), 4253–4269 (2016).

15. Agus F, Henson IE, Sahardjo BH, *et al.* Review of emission factors for assessment of CO2 emission from land use change to oil palm in Southeast Asia. *Reports from Tech. Panels 2nd Greenh. Gas Work. Gr. Roundtable Sustain. Palm Oil (RSPO)* [Internet]. , 7–28 (2013). Available from: http://www.rspo.org/file/GHGWG2/3_review_of_emission_factors_Agus_et_al.pdf.

16. Germer J, Sauerborn J. Estimation of the impact of oil palm plantation establishment on greenhouse gas balance. *Environ. Dev. Sustain.* 10(6), 697–716 (2008).

17. FAO. Crops processed; Indonesia and World total; Oil, palm; Production quantity; 2014. [Internet]. FAOSTAT. (2016). Available from: http://www.fao.org/faostat/en/?#data/QD.

18. Page SE, Rieley JO, Banks CJ. Global and regional importance of the tropical

peatland carbon pool. *Glob. Chang. Biol.* 17(2), 798–818 (2011).

19. Miettinen J, Hooijer A, Vernimmen R, Liew SC, Page SE. From carbon sink to carbon source: extensive peat oxidation in insular Southeast Asia since 1990. *Environ. Res. Lett.* [Internet]. 12(2), 24014 (2017). Available from: http://stacks.iop.org/1748-9326/12/i=2/a=024014?key=crossref.d5803ab4c180cc18647fc14663f0d775.

20. Hooijer A, Page S, Canadell JG, *et al.* Current and future CO 2 emissions from drained peatlands in Southeast Asia. *Biogeosciences*. 7(5), 1505–1514 (2010).

21. Miettinen J, Shi C, Liew SC. 2015 Land cover map of Southeast Asia at 250 m spatial resolution. *Remote Sens. Lett.* 7(7), 701–710 (2016).

22. Carlson KM, Curran LM, Asner GP, Pittman AM, Trigg SN, Marion Adeney J. Carbon emissions from forest conversion by Kalimantan oil palm plantations. *Nat. Clim. Chang.* [Internet]. 3(3), 283–287 (2012). Available from: http://www.nature.com/doifinder/10.1038/nclimate1702.

23. Gunarso P, Hartoyo ME, Agus F, Killeen TJ. Oil Palm and Land Use Change in Indonesia , Malaysia and Papua New Guinea. *Reports from Tech. Panels RSPOs 2nd Greenh. Gas Work. Gr.* , 29–64 (2013).

24. Koh LP, Miettinen J, Liew SC, Ghazoul J. Remotely sensed evidence of tropical peatland conversion to oil palm. *Proc. Natl. Acad. Sci.* [Internet]. 108(12), 5127–5132 (2011). Available from: http://www.pnas.org/cgi/doi/10.1073/pnas.1018776108.

25. Global Forest Watch. Oil palm concessions [Internet]. 2017. Available from: www.globalforestwatch.org.

26. ESA CCI. ESA CCI-Land Cover 2015 Product Users Guide Version 2.0 [Internet]. Available from: http://maps.elie.ucl.ac.be/CCI/viewer/download/ESACCI-LC-Ph2-PUGv2_2.0.pdf.

27. Miettinen J, Shi C, Tan WJ, Liew SC. 2010 land cover map of insular Southeast Asia in 250-m spatial resolution. *Remote Sens. Lett.* (2012).

28. Hansen MC, Potapov P V., Moore R, *et al.* High-Resolution Global Maps of 21st-Century Forest Cover Change. *Science (80-.).* [Internet]. 342(6160), 850–

853 (2013). Available from: http://www.sciencemag.org/cgi/doi/10.1126/science.1244693.

29. Margono BA, Potapov P V, Turubanova S, Stolle F, Hansen MC. Primary forest cover loss in Indonesia over 2000–2012. *Nat. Clim. Chang.* (2014).

30. Hargrove WW, Hoffman FM, Hessburg PF. Mapcurves: A quantitative method for comparing categorical maps. *J. Geogr. Syst.* 8(2), 187–208 (2006).

31. Khasanah N, van Noordwijk M, Ningsih H, Rahayu S. Carbon neutral? No change in mineral soil carbon stock under oil palm plantations derived from forest or non-forest in Indonesia. *Agric. Ecosyst. Environ.* [Internet]. 211, 195–206 (2015). Available from: http://dx.doi.org/10.1016/j.agee.2015.06.009.

32. IPCC. 2006 IPCC Guidelines for National Greenhouse Gas Inventories, Volume4: Agriculture, Forestry and Other Land Use. .

33. Ziegler AD, Phelps J, Yuen JQ, *et al.* Carbon outcomes of major land-cover transitions in SE Asia: Great uncertainties and REDD+ policy implications. *Glob. Chang. Biol.* (2012).

34. Agus F, Gunarso P, Sahardjo BH, Harris N, Noordwijk M Van, Killeen TJ. Historical Co 2 Emissions From Land Use and Land Use Change From the Oil Palm Industry in Indonesia , Malaysia and Papua New Guinea. , 65–88 (2010).

35. IPCC. 2006 IPCC Guidelines for National Greenhouse Gas Inventories [Internet]. Available from: https://www.ipcc-nggip.iges.or.jp/public/2006gl/.

36. Hooijer A, Page S, Jauhiainen J, *et al.* Subsidence and carbon loss in drained tropical peatlands. *Biogeosciences*. 9(3), 1053–1071 (2012).

37. Page SE, Siegert F, Rieley JO, Boehm H-D V, Jaya A, Limin S. The amount of carbon released from peat and forest fires in Indonesia during 1997. *Nature* [Internet]. 420, 61 (2002). Available from: http://dx.doi.org/10.1038/nature01131.

38. Moore S, Evans CD, Page SE, *et al.* Deep instability of deforested tropical peatlands revealed by fluvial organic carbon fluxes. *Nature* [Internet]. 493(7434), 660–663 (2013). Available from: http://dx.doi.org/10.1038/nature11818.

39. See LM, Fritz S. A method to compare and improve land cover Datasets:

Application to the GLC-2000 and MODIS land cover products. *IEEE Trans. Geosci. Remote Sens.* 44(7), 1740–1746 (2006).

40. Giri C, Zhu Z, Reed B. A comparative analysis of the Global Land Cover 2000 and MODIS land cover data sets. *Remote Sens. Environ.* 94(1), 123–132 (2005).

41. DeVisser MH, Messina JP. Optimum land cover products for use in a Glossina-morsitans habitat model of Kenya. *Int. J. Health Geogr.* [Internet]. 8(1), 39 (2009). Available from: http://ij-healthgeographics.biomedcentral.com/articles/10.1186/1476-072X-8-39.

42. Townshend J, Justice C, Li W, Gurney C, McManus J. Global land cover classification by remote sensing: present capabilities and future possibilities. *Remote Sens. Environ.* 35(2–3), 243–255 (1991).

43. Salomonson V V, Barnes W, Xiong J, Kempler S, Masuoka E. An overview of the Earth Observing System MODIS instrument and associated data systems performance. *IEEE Int. Geosci. Remote Sens. Symp.* 2(C), 1174–1176 (2002).

44. Roy DP, Wulder MA, Loveland TR, *et al.* Landsat-8: Science and product vision for terrestrial global change research. *Remote Sens. Environ.* 145, 154–172 (2014).

45. Whiteside T. a Comparison of Object-Oriented and Pixel-Based Classification Methods for Mapping Land Cover. (September), 1225–1231 (2005).

46. Myint SW, Gober P, Brazel A, Grossman-Clarke S, Weng Q. Per-pixel vs. object-based classification of urban land cover extraction using high spatial resolution imagery. *Remote Sens. Environ.* 115(5), 1145–1161 (2011).

47. Foody GM. Status of land cover classification accuracy assessment. *Remote Sens. Environ.* 80(1), 185–201 (2002).

48. Arnot C, Fisher P. Mapping the ecotone with fuzzy sets. In: *NATO Security through Science Series C: Environmental Security*. , 19–32 (2007).

49. Davis SJ, Burney JA, Pongratz J, Caldeira K. Methods for attributing land-use emissions to products. *Carbon Manag.* 5(2), 233–245 (2014).

50. The British Standards Institution; PAS 2050:2011; Specification for the assessment of the life cycle greenhouse gas emissions of goods and services. .

51. GanLian T, Cai H. Calculating GHG emission in oil palm using PalmGHG. *Planter*. 93(1092), 167–176 (2017).

52. Page SE, Banks CJ, Rieley JO. Tropical Peatlands: Distribution, Extent and Carbon Storage – Uncertainties and Knowledge Gaps. *Peatlands Int.* 2(2), 26–27 (2007).

53. Chaplin-Kramer R, Ramler I, Sharp R, *et al.* Degradation in carbon stocks near tropical forest edges. *Nat. Commun.* 6 (2015).

54. Brinck K, Fischer R, Groeneveld J, *et al.* High resolution analysis of tropical forest fragmentation and its impact on the global carbon cycle. *Nat. Commun.* 8 (2017).

55. Gregorio A Di, Henry M, Donegan E, *et al.* Classification Concepts Land Cover Classification System Software version 3. Available from: www.fao.org/.

Tables

Table 1 – Geographical extent and area of peat soil cover [19] and PO concessions [25] of the study areas

Province	Total area (ha)	Peat soil area (ha)	Peat (% of total area)	PO concession area (ha)	PO concession (% of total area)	PO on peat soil (ha)	PO on peat (% of total concession area)
North Sumatra	7,243,839	347,925	4.8	132,538	1.8	61,203	46.2
Riau	8,995,724	4,004,336	44.5	2,117,307	23.5	819,769	38.7
Central Kalimantan	15,354,930	3,005,097	19.6	3,199,420	20.8	464,079	14.5

Table 2 – Overview of LULC datasets used in this research

Organisation	**Acronym**	**Spatial resolution (m)**	**Spatial extent**	**Updates**	**URL data repository**
European Space Agency (ESA) Climate Change Initiative Land Cover	CCI	300 x 300	Global	Annual between 1992-2015	http://maps.elie.ucl.ac.be/CCI/viewer/
Centre for Remote Imaging, Sensing and Processing, Singapore	CRISP	250 x 250	Southeast Asia	2000, 2010, 2015	https://ormt-crisp.nus.edu.sg/ormt/Home/Disclaimer
Indonesia Ministry of Forestry	MoF	30x30 (100 x 100 used for this research)	Indonesia	1990, 1996, 2000, 2003, 2006, 2009, 2011, 2012, 2013, 2015	http://www.greenpeace.org/seasia/id/Global/seasia/Indonesia/Code/Forest-Map/en/index.html

Table 3 – Main contributors to LULC change for largest observed MoF LULC changes for all AOIs.

AOI	**Period**	**Total LULC change/yr (ha)**	**Largest LULC change/yr (ha)**	**From LULC class (t0) --> to LULC class (t1)**	**% of total**
North Sumatra	2006-2009	638,860	407,018	Dry Rice Land Mixed w/Scrub --> Dry Rice Land	63.7
Riau	2012-2013	1,118,233	726,066	Scrubland --> Dry Rice Land Mixed w/Scrub	64.9
Central Kalimantan	2013-2015	1,237,019	274,672	Scrubland --> Dry Rice Land Mixed w/Scrub	22.2

Table 4 – GHG emissions for three AOIs for 2000 - 2010/11, with % of emissions from mineral/peat

Emissions per year (Mg C yr^{-1}) and percent of total						
North Sumatra (4.8 % peat)						
	CCI (2000-2010)		CRISP (2000-2010)		MoF (2000-2011)	
Mineral	1,332,803	34.5	4,943,071	58.7	1,127,552	38.4
Peat	2,526,168	65.5	3,473,117	41.3	1,807,528	61.6
Total	*3,858,971*		*8,416,188*		*2,935,080*	
Riau (44.5 % peat)						
	CCI (2000-2010)		CRISP (2000-2010)		MoF (2000-2011)	
Mineral	9,533,167	33.2	11,784,303	28.7	4,812,749	17.2
Peat	19,174,983	66.8	29,246,758	71.3	23,105,593	82.8
Total	*28,708,150*		*41,031,060*		*27,918,343*	
Central Kalimantan (19.6 % peat)						
	CCI (2000-2010)		CRISP (2000-2010)		MoF (2000-2011)	
Mineral	6,699,626	62.3	14,791,021	55.9	8,275,277	61.7
Peat	4,055,275	37.7	11,693,997	44.2	5,142,602	38.3
Total	*10,754,901*		*26,485,018*		*13,417,880*	

Table 5 – GHG emissions for three AOIs for 2010/11 - 2015, with % of emissions from mineral/peat

Emissions per year (Mg C yr^{-1}) and percent of total				
North Sumatra (4.8 % peat)				
	CCI (2010-2015)		MoF (2011-2015)	
Mineral	491,500	47.8	3,450,122	80.3
Peat	536,465	52.2	845,314	19.7
Total	*1,027,966*		*4,295,435*	
Riau (44.5 % peat)				
	CCI (2010-2015)		MoF (2011-2015)	
Mineral	4,055,092	32.12	6,200,630	27.1
Peat	8,571,629	67.88	16,672,805	72.9
Total	*12,626,721*		*22,873,435*	
Central Kalimantan (19.6 % peat)				
	CCI (2010-2015)		MoF (2011-2015)	
Mineral	2,814,481	58.5	10,357,934	48.6
Peat	1,994,610	41.5	10,941,092	51.4
Total	*4,809,091*		*21,299,027*	

Figures

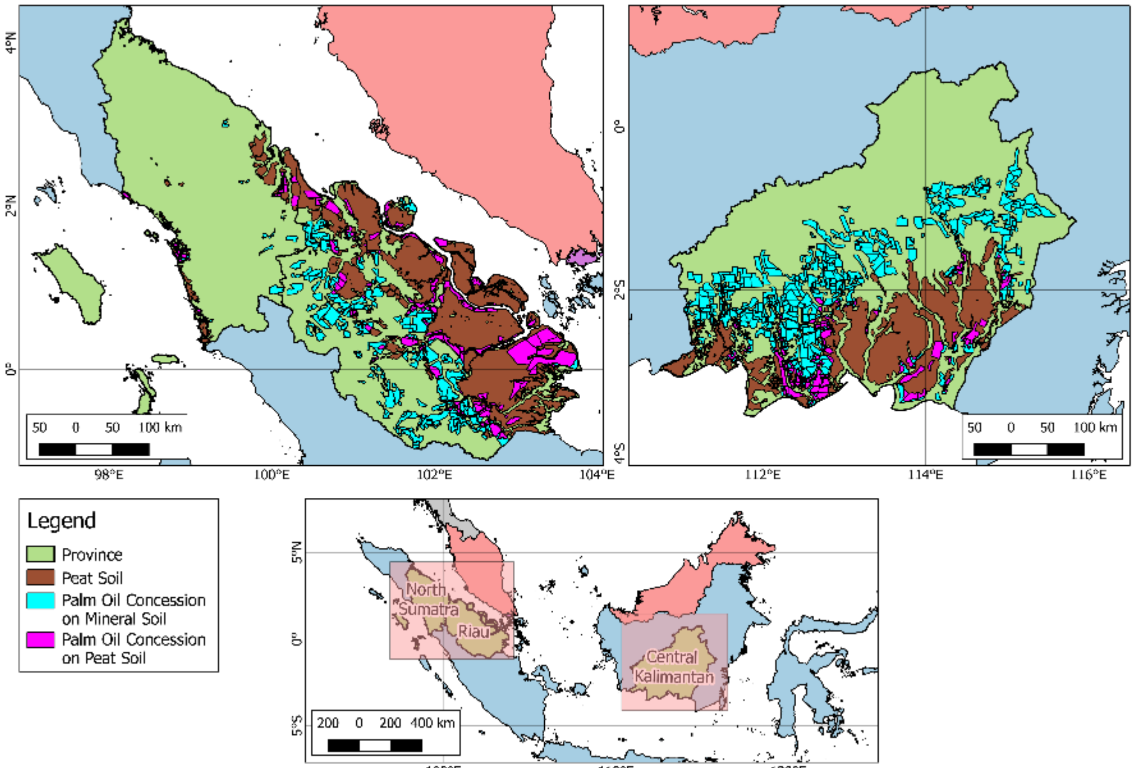

Figure 1

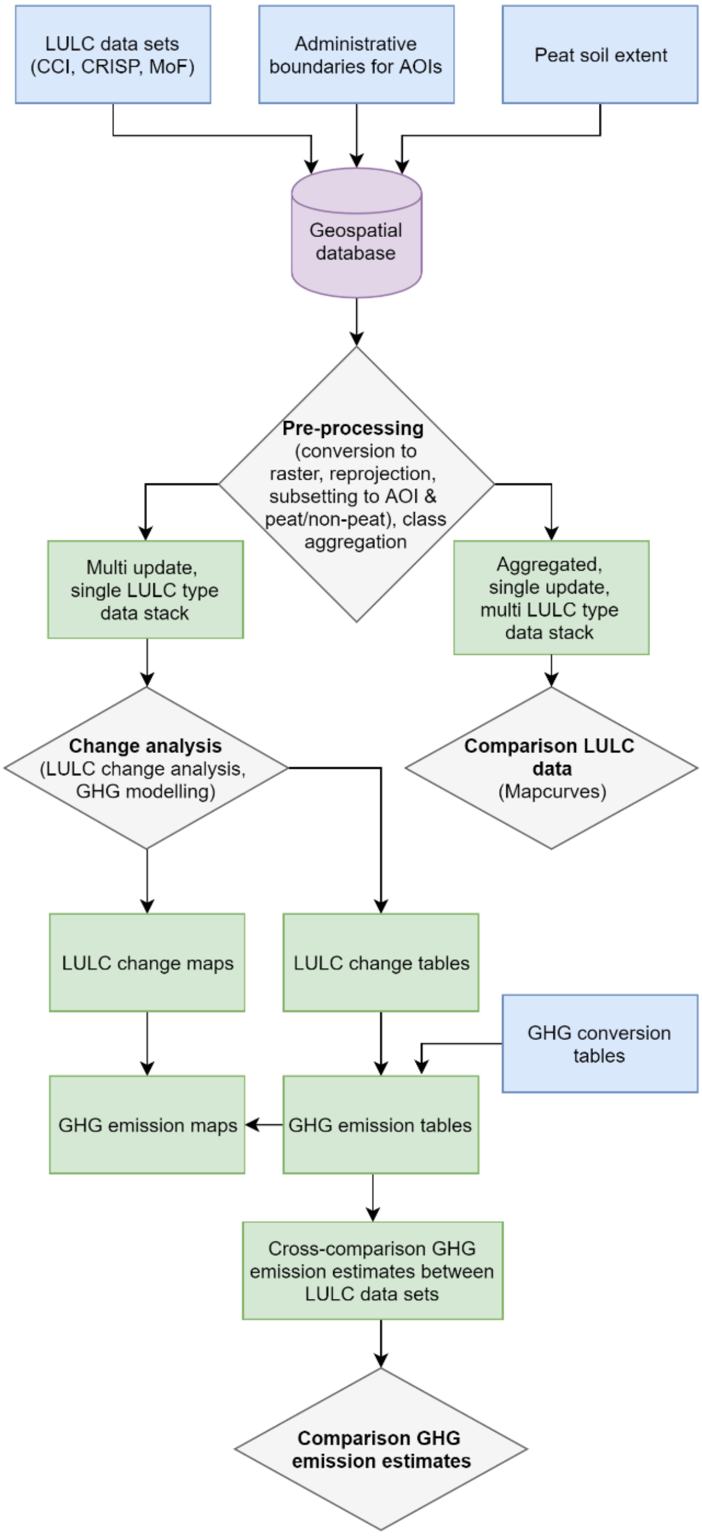
LULC data sets
(CCI, CRISP, MoF)
Administrative boundaries for AOIs
Peat soil extent
Geospatial database
Pre-processing
(conversion to raster, reprojection, subsetting to AOI & peat/non-peat), class aggregation
Multi update, single LULC type data stack
Aggregated, single update, multi LULC type data stack
Change analysis
(LULC change analysis, GHG modelling)
Comparison LULC data
(Mapcurves)
LULC change maps
LULC change tables
GHG conversion tables
GHG emission maps
GHG emission tables
Cross-comparison GHG emission estimates between LULC data sets
Comparison GHG emission estimates

Figure 2

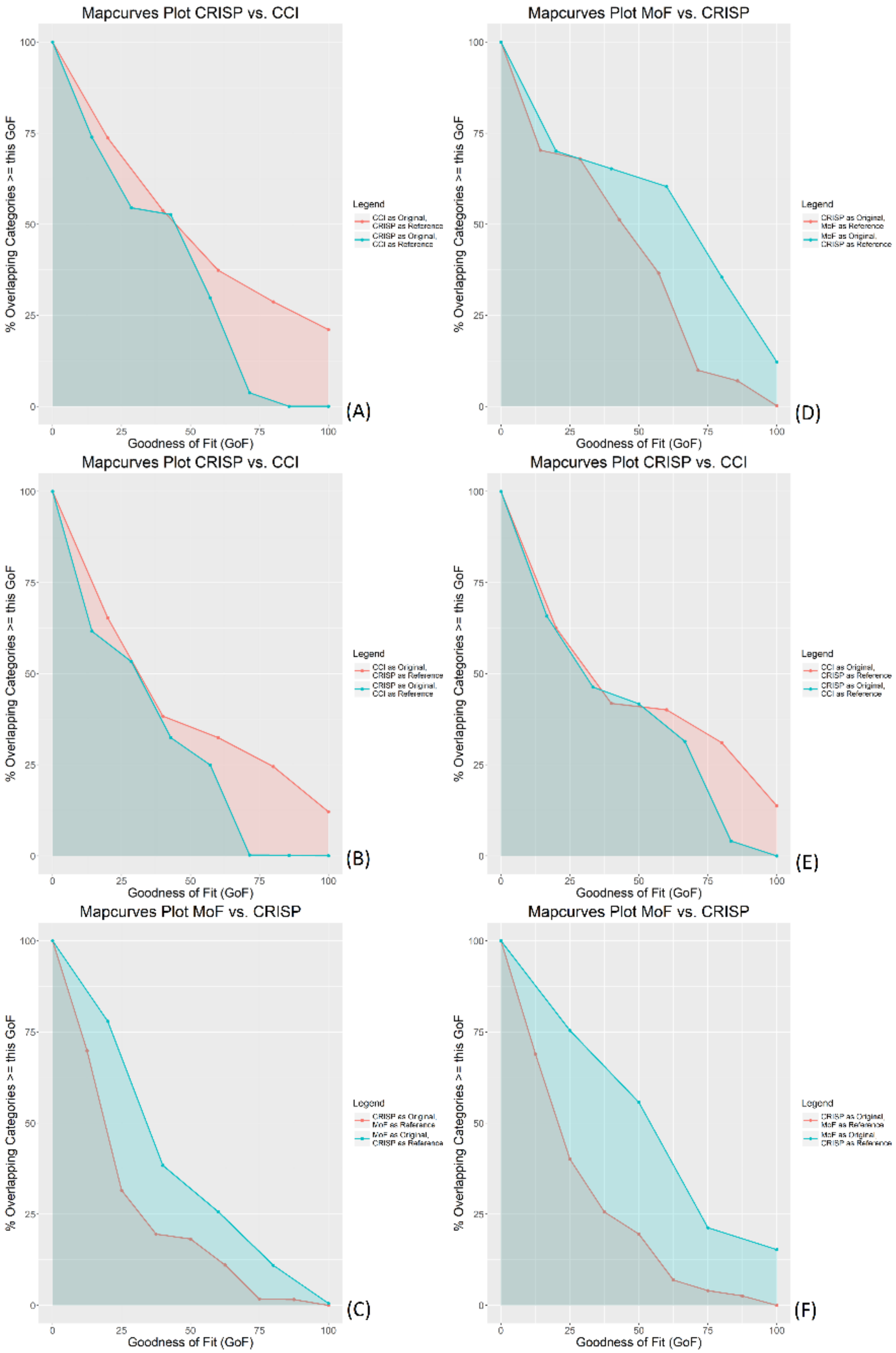
Mapcurves Plot CRISP vs. CCI
% Overlapping Categories >= this GoF
Goodness of Fit (GoF)
Legend
CCI as Original, CRISP as Reference
CRISP as Original, CCI as Reference
(A)
Mapcurves Plot MoF vs. CRISP
% Overlapping Categories >= this GoF
Goodness of Fit (GoF)
Legend
CRISP as Original, MoF as Reference
MoF as Original, CRISP as Reference
(D)
Mapcurves Plot CRISP vs. CCI
% Overlapping Categories >= this GoF
Goodness of Fit (GoF)
Legend
CCI as Original, CRISP as Reference
CRISP as Original, CCI as Reference
(B)
Mapcurves Plot CRISP vs. CCI
% Overlapping Categories >= this GoF
Goodness of Fit (GoF)
Legend
CCI as Original, CRISP as Reference
CRISP as Original, CCI as Reference
(E)
Mapcurves Plot MoF vs. CRISP
% Overlapping Categories >= this GoF
Goodness of Fit (GoF)
Legend
CRISP as Original, MoF as Reference
MoF as Original, CRISP as Reference
(C)
Mapcurves Plot MoF vs. CRISP
% Overlapping Categories >= this GoF
Goodness of Fit (GoF)
Legend
CRISP as Original, MoF as Reference
MoF as Original, CRISP as Reference
(F)

Figure 3

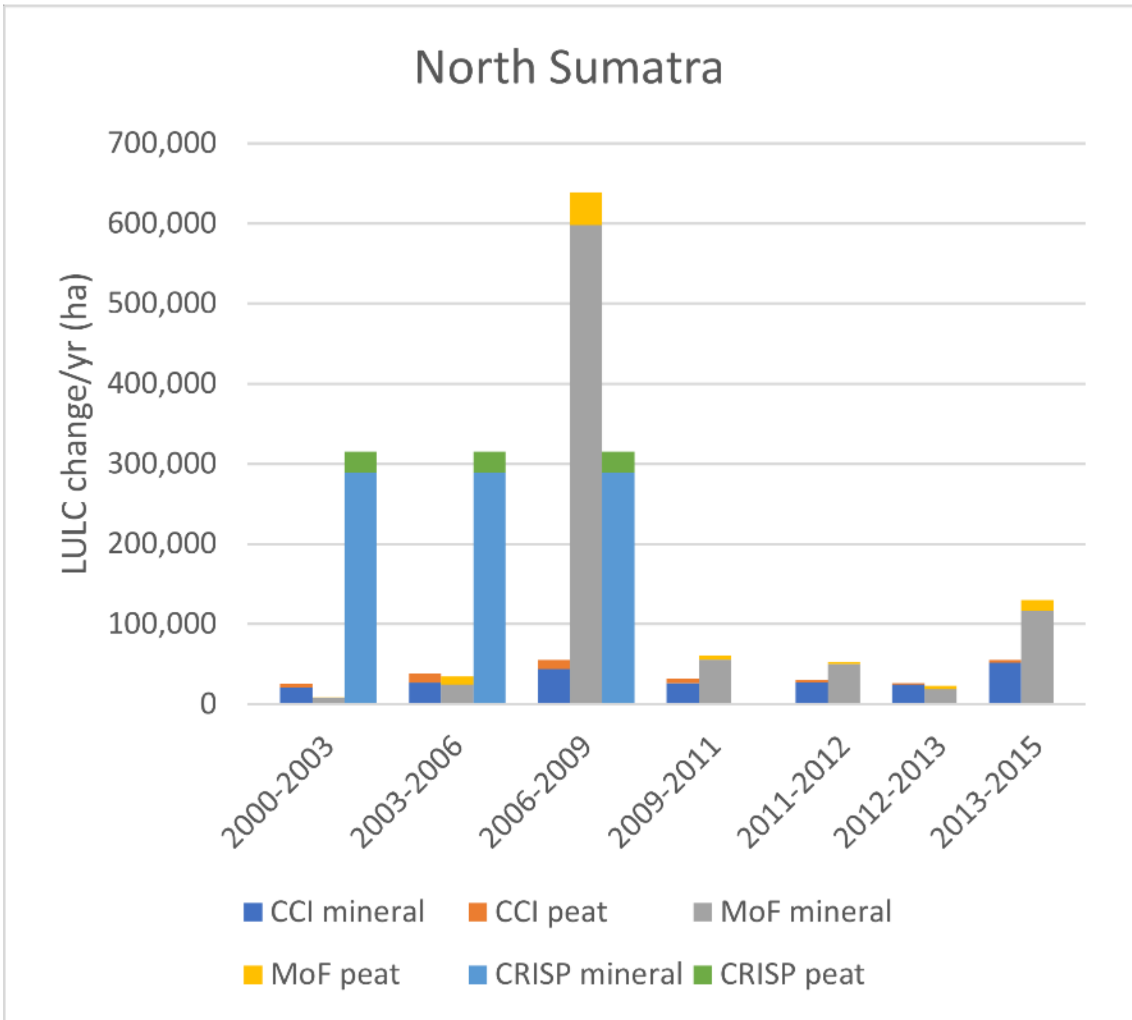
North Sumatra
LULC change/yr (ha)
700,000
600,000
500,000
400,000
300,000
200,000
100,000
0
2000-2003
2003-2006
2006-2009
2009-2011
2011-2012
2012-2013
2013-2015
CCI mineral
CCI peat
MoF mineral
MoF peat
CRISP mineral
CRISP peat

Figure 4

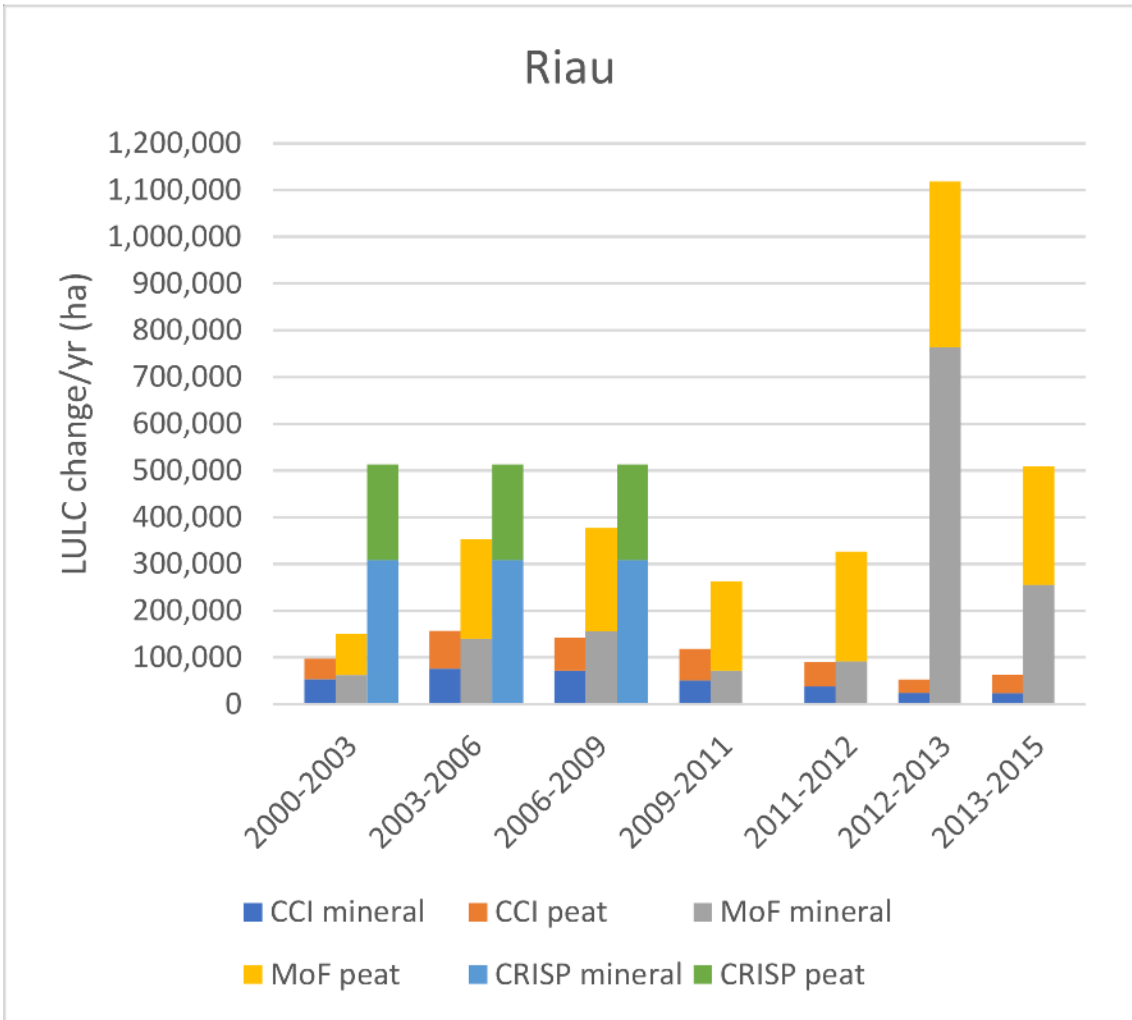
Riau
LULC change/yr (ha)
1,200,000
1,100,000
1,000,000
900,000
800,000
700,000
600,000
500,000
400,000
300,000
200,000
100,000
0
2000-2003
2003-2006
2006-2009
2009-2011
2011-2012
2012-2013
2013-2015
CCI mineral
CCI peat
MoF mineral
MoF peat
CRISP mineral
CRISP peat

Figure 5

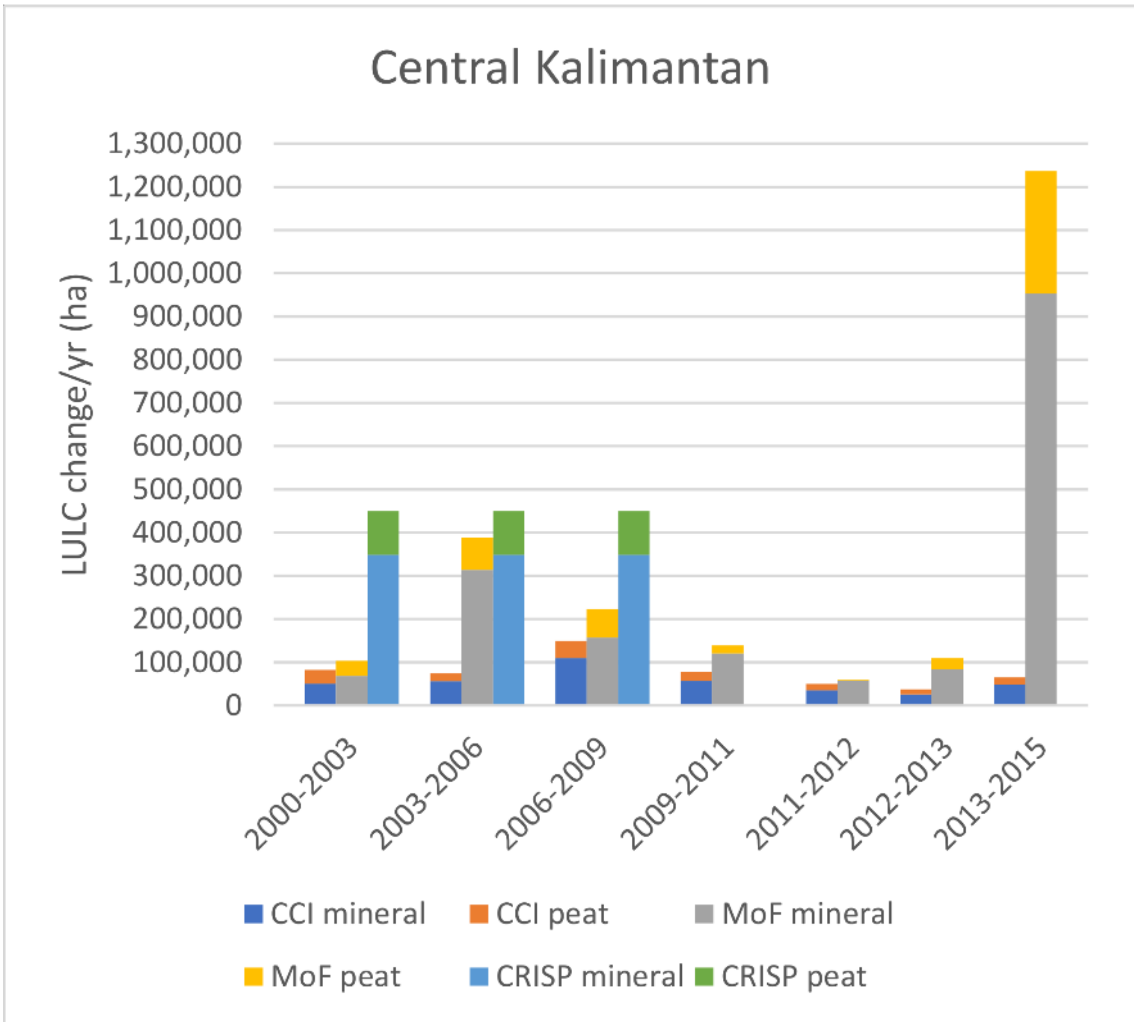
Central Kalimantan
LULC change/yr (ha)
1,300,000
1,200,000
1,100,000
1,000,000
900,000
800,000
700,000
600,000
500,000
400,000
300,000
200,000
100,000
0
2000-2003
2003-2006
2006-2009
2009-2011
2011-2012
2012-2013
2013-2015
CCI mineral
CCI peat
MoF mineral
MoF peat
CRISP mineral
CRISP peat

Figure 6

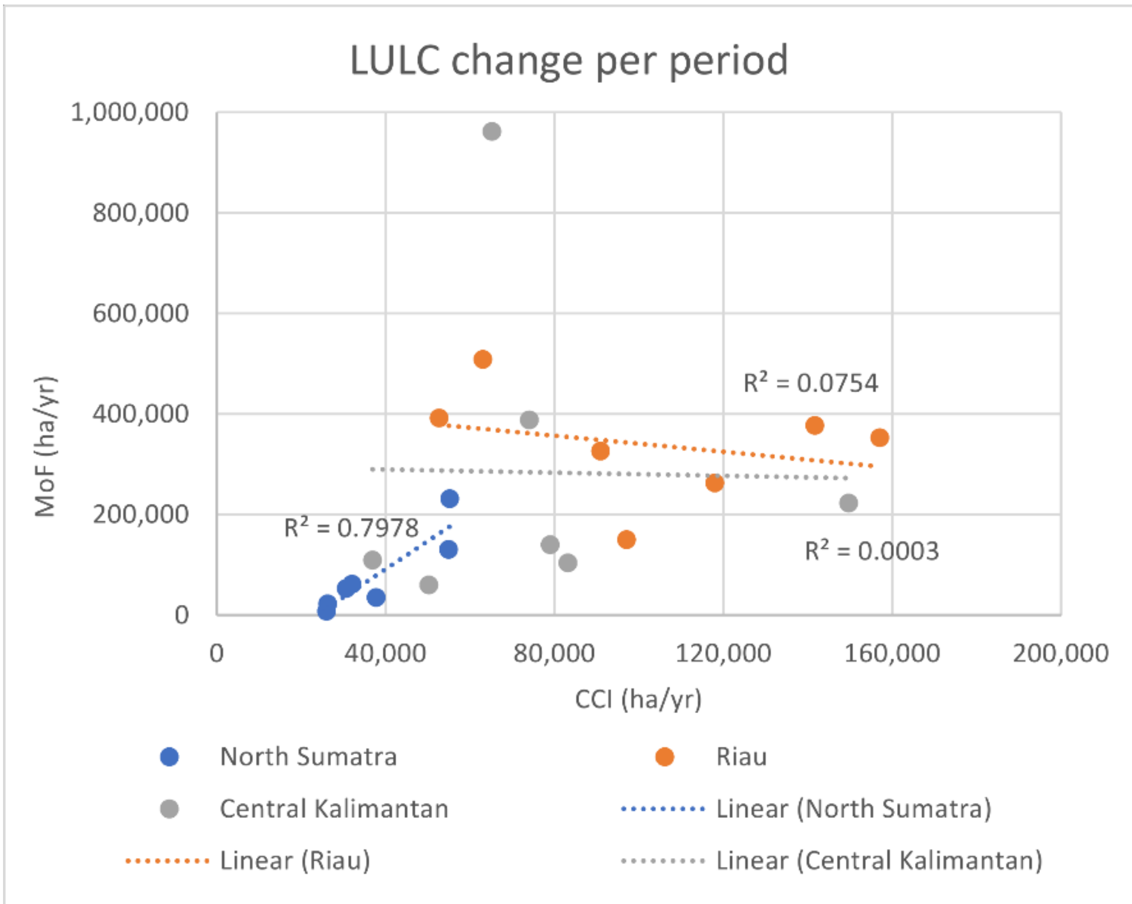
LULC change per period
1,000,000
800,000
600,000
400,000
200,000
0
MoF (ha/yr)
0
40,000
80,000
120,000
160,000
200,000
CCI (ha/yr)
R² = 0.7978
R² = 0.0754
R² = 0.0003
North Sumatra
Riau
Central Kalimantan
Linear (North Sumatra)
Linear (Riau)
Linear (Central Kalimantan)

Figure 7

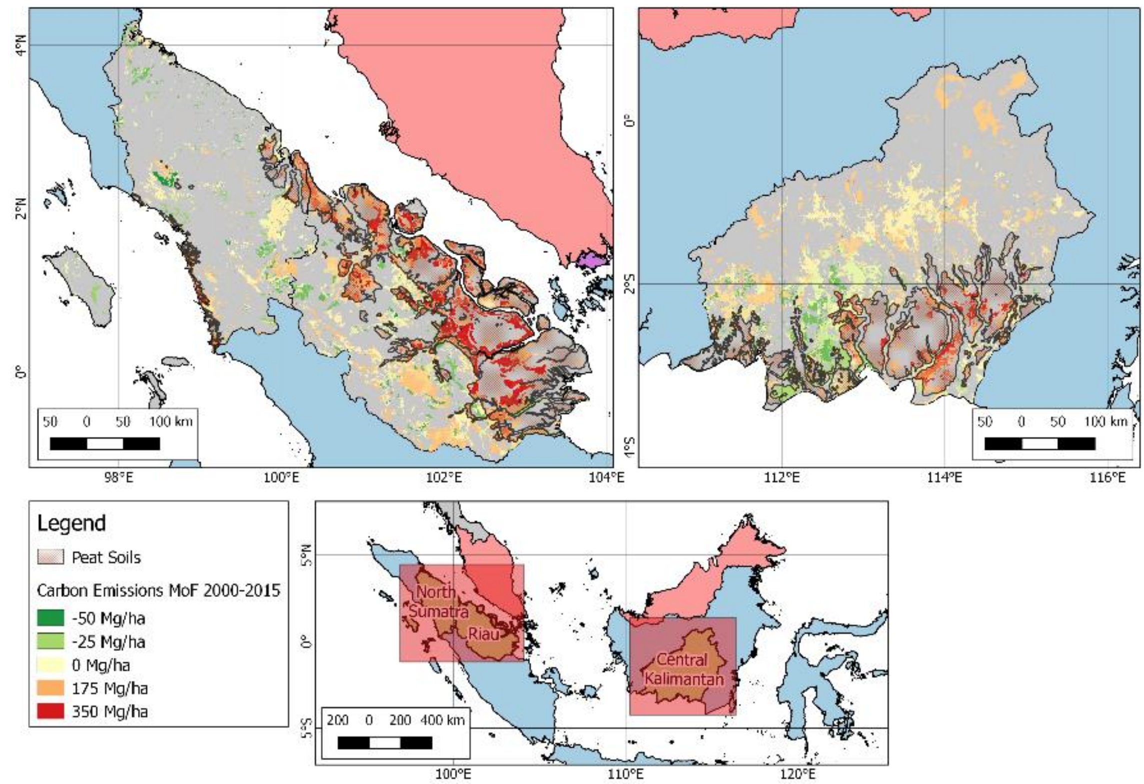

Legend
Peat Soils
Carbon Emissions MoF 2000-2015
-50 Mg/ha
-25 Mg/ha
0 Mg/ha
175 Mg/ha
350 Mg/ha
North Sumatra
Riau
Central Kalimantan
50 0 50 100 km
200 0 200 400 km
98°E
100°E
102°E
104°E
112°E
114°E
116°E
110°E
120°E
4°N
2°N
0°
2°S
4°S
5°N
5°S

Figure 8

Figure captions

Figure 1 - The AOIs in Indonesia, with PO plantation concessions and peat soil areas indicated.

Figure 2 - Data analysis workflow diagram

Figure 3 – Best fitting mapcurve plots for North Sumatra (3a and 3d), Riau (3b and 3e) and Central Kalimantan (3c and 3f) for 2000 and 2015, respectively

Figure 4 - LULC change in North Sumatra between 2000 and 2015

Figure 5 - LULC change in Riau between 2000 and 2015

Figure 6 - LULC change in Central Kalimantan between 2000 and 2015

Figure 7 – Scatter plot LULC change estimates in all three AOIs in the period 2000-2015 from CCI and MoF

Figure 8 - GHG emission map of AOIs, based on MoF data for the period 2000-2015